Online-Journals.org

iJET International Journal of Emerging Technologies in Learning

iJET | eISSN: 1863-0383 | Vol. 18 No. 20 (2023) | OPEN ACCESS

https://doi.org/10.3991/ijet.v18i20.44209

PAPER

Virtual Reality and Augmented Reality for Immersive Learning: A Framework of Education Environment Design

Biqin Yang(✉)

School of Business,
Minnan Normal University,
Zhangzhou, China

yangbiqin1987@163.com

ABSTRACT

The technologies of virtual reality (VR) and augmented reality (AR) have developed fast in recent years and have been applied in various scenarios, including the field of education. Now educators attempt to make use of these new technologies to create an immersive learning environment (ILE) for students, in the hopes of helping them improve learning efficiency and quality. Currently, available research on the design and optimization of ILE focus on how to introduce teaching content into the 3D environment and improve user experience, while a series of problems are still pending for solutions, such as how to arrange the layout in multi-dimensional space, how to optimize the vision in immersive environment based on edge strategy, and how to improve image quality using panoramic-view specific-region super-resolution (PSS) algorithms that use non-local feature fusion. In view of these matters, this study proposed a novel method for the design and optimization of an ILE. At first, problems of how to create a visual layout of network topology in the ILE, how to arrange the layout based on the advantages of different-dimensional spaces in scenes, and how to carry out visual optimization combined with the edge strategy were discussed in detail. Then, a new PSS algorithm that utilizes non-local feature fusion was proposed, and the functioning of the multi-scale non-local feature fusion module and the specific structure of the high-solution network were introduced in detail. The findings of this study could provide useful theoretical evidences and practical guidance for the design and optimization of ILE, giving new possibilities for improving the effect of ILE and enhancing user experience.

KEYWORDS

immersive learning environment (ILE), network topology, visual layout, edge strategy, visual optimization, non-local feature fusion, panoramic view specific-region super resolution algorithm (PSS)

Yang, B. (2023). Virtual Reality and Augmented Reality for Immersive Learning: A Framework of Education Environment Design. *International Journal of Emerging Technologies in Learning (iJET)*, 18(20), pp. 23–36. https://doi.org/10.3991/ijet.v18i20.44209

Article submitted 2023-06-20. Revision uploaded 2023-08-11. Final acceptance 2023-08-21.

1 INTRODUCTION

As a new round of technological revolution is coming, technologies such as virtual reality (VR) [1–3] and augmented reality (AR) [4–7] are now transforming our way of life and working as a brand new method of perception and interaction that transcends images, texts, and videos and opens a whole new 3D world for us. In the field of education, they also open up new possibilities [8–13].

In a traditional teaching environment, students are usually stuck with two-dimensional textbooks and learning resources. For some complicated concepts, they are unable to understand or master them from different perspectives and dimensions [14–17]. For instance, some students often find it difficult to understand and master abstract mathematical concepts and physical principles. With the help of VR and AR, these complex concepts can be shown in 3D space, where students can view them from various perspectives and dimensions, and this can improve their learning efficiency and quality [18–20].

An immersive learning environment (ILE) not only provides new learning resources but also changes the way people learn. In such an environment, students can interact with the environment, seek knowledge by themselves, and build their own knowledge structure, while in contrast, in a traditional learning environment, they just receive knowledge passively. A good example is the virtual lab. Students can perform experiments in the virtual lab and experience the history in a simulated historical scene. This can deepen students' learning, increase the pertinence of learning, and trigger students' learning interest.

However, despite the fact that ILE has unlimited potential, there are many challenges in its actual design and application, such as the problems of how to effectively utilize the 3D space, how to realize effective visual optimization in the immersive environment [21–23], and how to effectively merge the teaching content into the immersive environment [24] [25].

The purpose of this research is to discuss the design methods and application strategies of ILEs. At first, the visual layout of network topology in ILEs was investigated, and a few problems were studied, including how to arrange the layout based on the advantages of different-dimensional spaces in scenes and how to carry out visual optimization combining with the edge strategy so as to improve learning environment and user experience. After that, a PSS algorithm provides a new idea and method for image processing and rendering of immersive learning environments.

2 VISUAL LAYOUT OF IMMERSIVE-STYLE NETWORK TOPOLOGY

The visual layout of network topology plays an important role in ILE as it can help create a learning environment that conforms to cognitive laws and improves the efficiency of information acquisition and processing. Through an in-depth investigation on how to arrange layout based on the advantages of different-dimensional spaces in scenes, an environment that is closer to the cognitive pattern of learners can be created, so that the learners can acquire and process information more naturally and intuitively in the VR or AR environment. Figure 1 gives the framework for the design of an immersive learning environment.

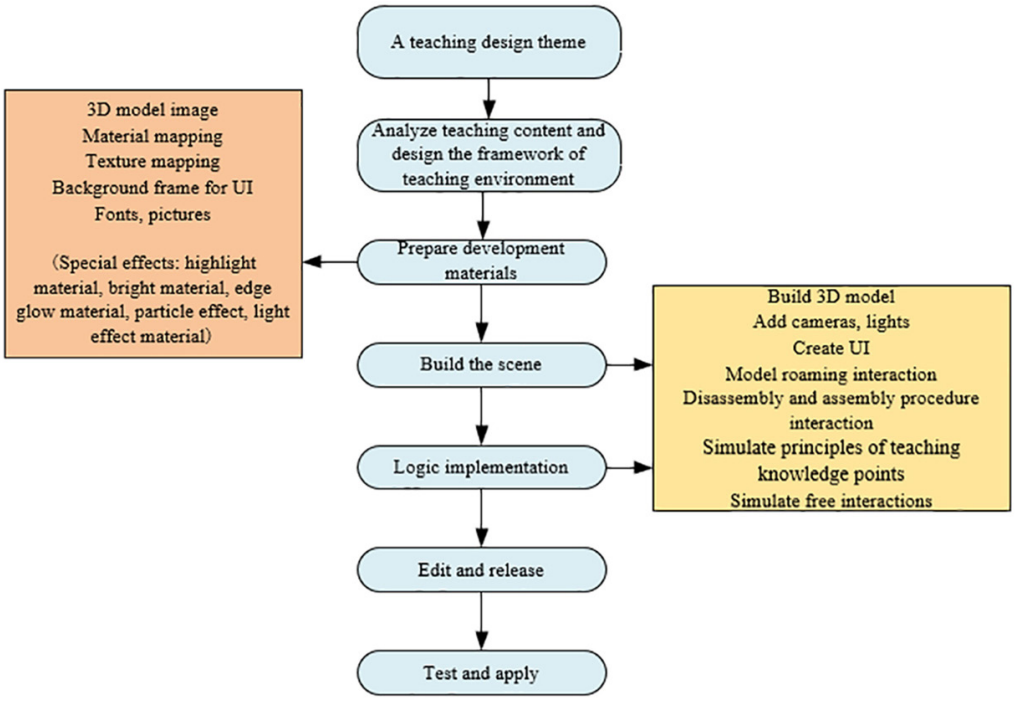

Fig. 1. Framework of immersive learning environment design

There are some challenges in the analysis of the network topology of an ILE, and the first one is the complexity of the ILE itself. Since an immersive environment has a higher sense of reality and is more interactive, the visual layout of network topology needs to take more dimensions and factors into consideration, such as spatial layout, user perspective, interaction mode, etc., and these have posed new requirements for the analysis of network topology. Another challenge is how to use the ILE to carry out analysis when facing large-scale and complex network data, and this requires researchers to develop new visualization techniques and algorithms to improve data processing efficiency and accuracy.

The dimension-fusion network topology layout is an effective method to solve the analysis of network topology in ILE, it can make full use of the advantages of different dimensional spaces to compensate for the shortcomings of single-dimension layout, thereby improving the understanding and analysis of the network. The single-dimension of the layout can help users perceive network relevance as a whole; however, due to the limited dimension of layout, its ability to explore deep into the internal relevance of communities is relatively weak, which has restricted users' deeper level understanding and analysis of the network. In contrast, the dimension-fusion network topology layout introduces more dimensions based on the one-dimension layout, enabling the users to observe and analyze the network from different perspectives and levels, thereby making explorations step-by-step from the overall perspective to the details at each level. The community structure partitioning method based on the modularity matrix and the dimension fusion layout based on the Fruchterman Reingold (FR) algorithm are two important approaches for processing the network topology, and both are playing important roles in improving the visual effect of the network and interpreting the complex network structure. In this paper, the two methods were combined to realize a dimension-fusion network topology layout in an ILE. Figure 2 illustrates the flow of the dimension transformation topology layout.

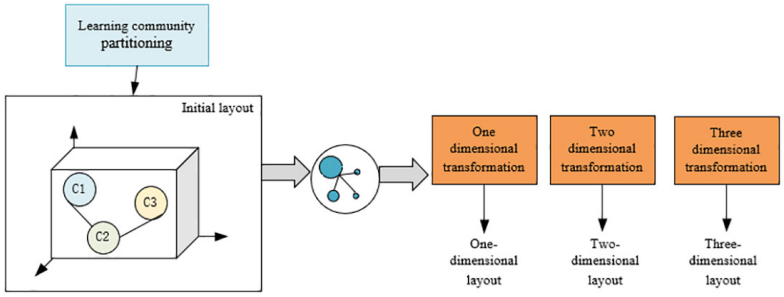

Fig. 2. Flow of dimension transformation topology layout

The community structure partitioning method based on the modularity matrix uses the modularity matrix of the network to reveal the potential mode between community structure and its features. This method draws on the concept of modularity matrix proposed by NewMan to perform community partitioning on network structure and find the benefit function that maximizes the network modularity, thereby realizing effective identification of community structure in the network. Network modularity means that a network is partitioned into multiple, relatively independent modules or communities that are densely connected internally and sparsely connected externally. Modularity maximization is to search for the optimal solution of network partitioning so that the number of links inside communities is the highest and the number of links between communities is the lowest. Such community partitioning is conducive to revealing the community structure of the network, as it provides a clearer view to help users understand and analyze the internal structure and functions of the network.

Assuming there are b nodes and l edges in a network, where F_c represents the degree of any node c in the network, and the network is represented by an undirected graph adjacency matrix S. If there is a connecting edge between two nodes c_u and c_k, then S_{uk} is equal to 1, otherwise it is equal to 0. In the process of randomly assigning edges to the network, the edges need to be bisected to generate $l_b = 2l$ connecting points; in a network in which $2l$ connecting points are randomly matched, the expected value of the probability of the number of connecting edges between c_u and c_k can be represented by $EX_{uk} = F_u F_k / 2l$, then in the random network, the difference between the number of connecting edges between c_u and c_k and the expected value of the probability of the number of connecting edges between the two can be represented by $S_{uk} - EX_{uk}$; assuming $F_u F_k / 2l = O_{uk}$ represents the probability model of nodes c_u and c_k about edges; σ_{uk} represents whether nodes c_u and c_k belong to a same community, and its quantified expression is $\sigma_{uk} = (A_{uk} + m)/2$, then the following formula gives the expression of modularity:

$$W = \frac{1}{2l} \sum_{uk} \left[S_{uk} - \frac{F_u F_k}{2l} \right] \sigma_{uk} \tag{1}$$

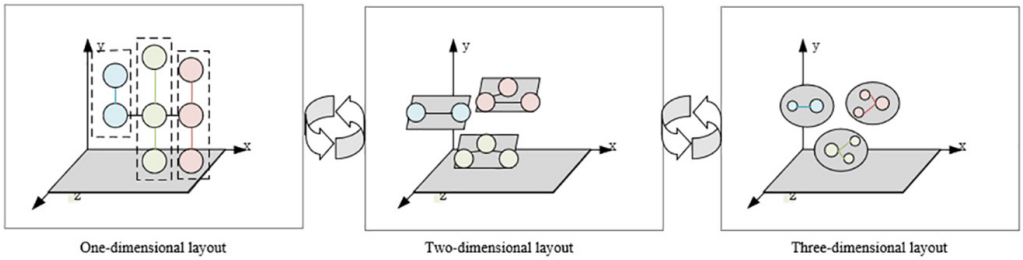

Fig. 3. Visual layout of different dimensions

The dimension fusion layout based on the FR algorithm draws on the idea of the FR algorithm based on the partitioning results of the previous method and integrates the layout of different dimensions into an immersive 3D environment. The FR algorithm is a commonly used force-directed layout algorithm that arranges the layout of network nodes by stimulating the interaction of forces, thereby attaining a good visual effect of the network. In an immersive environment, the FR algorithm can effectively reduce chaotic nodes and crossing edges so that the visual effect of the network can be shown better. By introducing 3D space, it can give richer information about the network structure and provide a more intuitive and natural way of interaction, thereby further improving the users' learning and using experience. Figure 3 shows the visual layout of different dimensions. Assuming $f(u, k)$ represents the distance between nodes u and j, $a(u, k)$ represents the length of the spring model, k represents the elasticity coefficient of the spring model, r represents the electrostatic force constant between any nodes, μ represents the weight between the two nodes, then the following formula gives the definition of the energy model in the FR algorithm:

$$R = \sum_{u=1}^{b}\sum_{k=1}^{b}\frac{1}{2}j[f(u,k)-a(u,k)]^2 + \sum_{u=1}^{b}\sum_{k=1}^{b}\frac{e\mu_{uk}}{f(u,k)^2} \tag{2}$$

In order to fully retain the structural features of learning communities in the ILE, after being subjected to the force-directed layout, the coordinates (z_u, t_u, x_u) of super node V_u were taken as the center to perform the secondary force-directed layout; assuming (y_z, y_t, y_x) represents the spatial translation vector, then the spatial translation transformation matrix can be written as:

$$Y(y) = Y(y_z, y_t, y_x) = \begin{bmatrix} 1 & 0 & 0 & y_z \\ 0 & 1 & 0 & y_t \\ 0 & 0 & 1 & y_x \\ 0 & 0 & 0 & 1 \end{bmatrix} \tag{3}$$

Assuming: (z, t, x) represents the coordinates of any node after subjected to the secondary force-directed layout, $[z_u\, t_u\, z\ 1]^Y$ represents the one-dimensional homogeneous coordinate matrix of the node, $[z_u\, t\, x\ 1]^T$ represents the two-dimensional homogeneous coordinate matrix of the node, $[z\ t\ x\ 1]^T$ represents the three-dimensional homogeneous coordinate matrix of the node, then the following formula gives the expression of the homogeneous coordinate matrix of transformed c in any spatial dimension:

$$P(*) = \begin{cases} Y(y)\times\left[z_u\ \ t_u\ \ z\ \ 1\right]^T, if\ \ 1F \\ Y(y)\times\left[z_u\ \ t\ \ x\ \ 1\right]^T, if\ \ 2F \\ Y(y)\times\left[z\ \ t\ \ x\ \ 1\right]^T, if\ \ 3F \end{cases} = \begin{bmatrix} z^* \\ t^* \\ x^* \\ 1 \end{bmatrix} \tag{4}$$

3 PSS ALGORITHM FOR IMMERSIVE LEARNING ENVIRONMENT

The PSS algorithm based on non-local feature fusion is very meaningful for the design of an ILE. The image quality of the ILE directly affects the learning experience of learners, and the proposed PSS algorithm based on non-local feature fusion can greatly improve the said image quality, making the created ILE more vivid, thereby

enriching learners' perception experience and increasing their learning initiative and interest.

The proposed algorithm aims at the super-resolution reconstruction of specific regions in panoramic view images of the ILE and to improve the visual experience of users. In terms of the adaptive feature fusion of non-local networks, the proposed algorithm can automatically identify and fuse features in different regions of panoramic view images and provide richer information sources for super-resolution reconstruction. The conventional super-resolution reconstruction methods tend to consider only the local pixel information, while the global features of images are often ignored. Non-local networks can improve the accuracy of super-resolution reconstruction through global feature fusion, as they can improve the resolution of specific surrounding regions by fusing non-local features in images based on the high resolution of the viewport of panoramic view images.

Assuming: t_u represents output response of the position to be calculated, z represents the input feature image, k represents the position index of the input feature image, $Va(z)$ represents the normalization factor, d represents the function for calculating the similarity between two specific feature blocks, Q_h represents the matrix to be learnt, then the general formula for non-local networks is:

$$tu_i = \frac{1}{V(z)} \sum_{\forall k} d(z_u, z_k) h(z_k) \tag{5}$$

$$h(z_k) = Q_h z_u \tag{6}$$

To improve the accuracy and comprehensiveness of the fused information of high resolution viewport, this paper proposed a multi-scale non-local feature fusion method. Assuming, U^{ME} represents low resolution region, U^{RE} represents high resolution viewport, then with the help of this method, the dependency matrix between U^{ME} and U^{RE} can be calculated, then, based on the attained dependency matrix, U^{RE} was adaptively fused into U^{ME}. Assuming: $\phi(\cdot)$ and $\theta(\cdot)$ are convolution kernels with a size of 1×1, which were used to map the high-level semantic features U_{chh}^{ME} and $U_{chh}^{RE\downarrow}$ of regions U^{ME} and U^{RE} extracted by the deep learning network into a feature image with a size of $[v/2, g, q]$; based on the embedded Gaussian function, the similarity between image blocks can be quantified:

$$d(z_u, z_k) = e^{\varphi(z_u) Y \theta(z_k)} \tag{7}$$

$$\varphi(z_u) = Q_\varphi z_u \tag{8}$$

$$\theta(z_u) = Q_\theta z_u \tag{9}$$

Through the mapping of $\phi(\cdot)$ and $\theta(\cdot)$, U_{chh}^{ME} and $U_{chh}^{RE\downarrow}$ cut the number of channels in half. $\phi\left(U_{chh}^{ME}\right)$ was stretched and transformed into a two-dimensional matrix with a size of $[v/2, g \times q]$, $\theta\left(U_{chh}^{RE\downarrow}\right)$ was used to stretch and transpose $U_{chh}^{RE\downarrow}$ to get a two-dimensional matrix with a size of $[g \times q, v/2]$, and the final dependency matrix L was attained by multiplying the two. L characterizes the global similarity between U_{chh}^{ME} and $U_{chh}^{RE\downarrow}$, and its calculation formula is:

$$L_u = \frac{1}{\sum_{\forall k} e^{\varphi\left(U_u^{ME}\right)^Y \theta\left(U_k^{RE}\right)}} e^{\varphi\left(U_u^{ME}\right)^Y \theta\left(U_k^{RE}\right)} Q_h x_k \tag{10}$$

The super-resolution network proposed in this study mainly consists of a gradient-guided branch and a super-resolution branch. The super-resolution branch takes the residual network as its main structure, as this structure can effectively decrease the training difficulty of deep networks and improve their stability and performance. On this basis, by using the dependency matrix *M* to adaptively fuse the content of the high-resolution viewport, the network is able to make full use of the high-resolution information for super-resolution reconstruction. The super-resolution branch fuses the output of the upsampling layer with features of the gradient-guided branch; this step can improve the quality of the details of the reconstructed image so that it could be more realistic and detailed. Then, to further improve the quality of edge details, the gradient-guided branch was introduced, aiming at correcting and optimizing the high-frequency detail information of the reconstructed super-resolution image. Considering that the super-resolution branch can carry rich structural information, which is conducive to the restoration of gradient maps, so in the gradient branch, intermediate feature results coming from the super-resolution branch will be fused to improve the guidance accuracy of the gradient-guided branch. Figure 4 shows the overall framework of the super-resolution network.

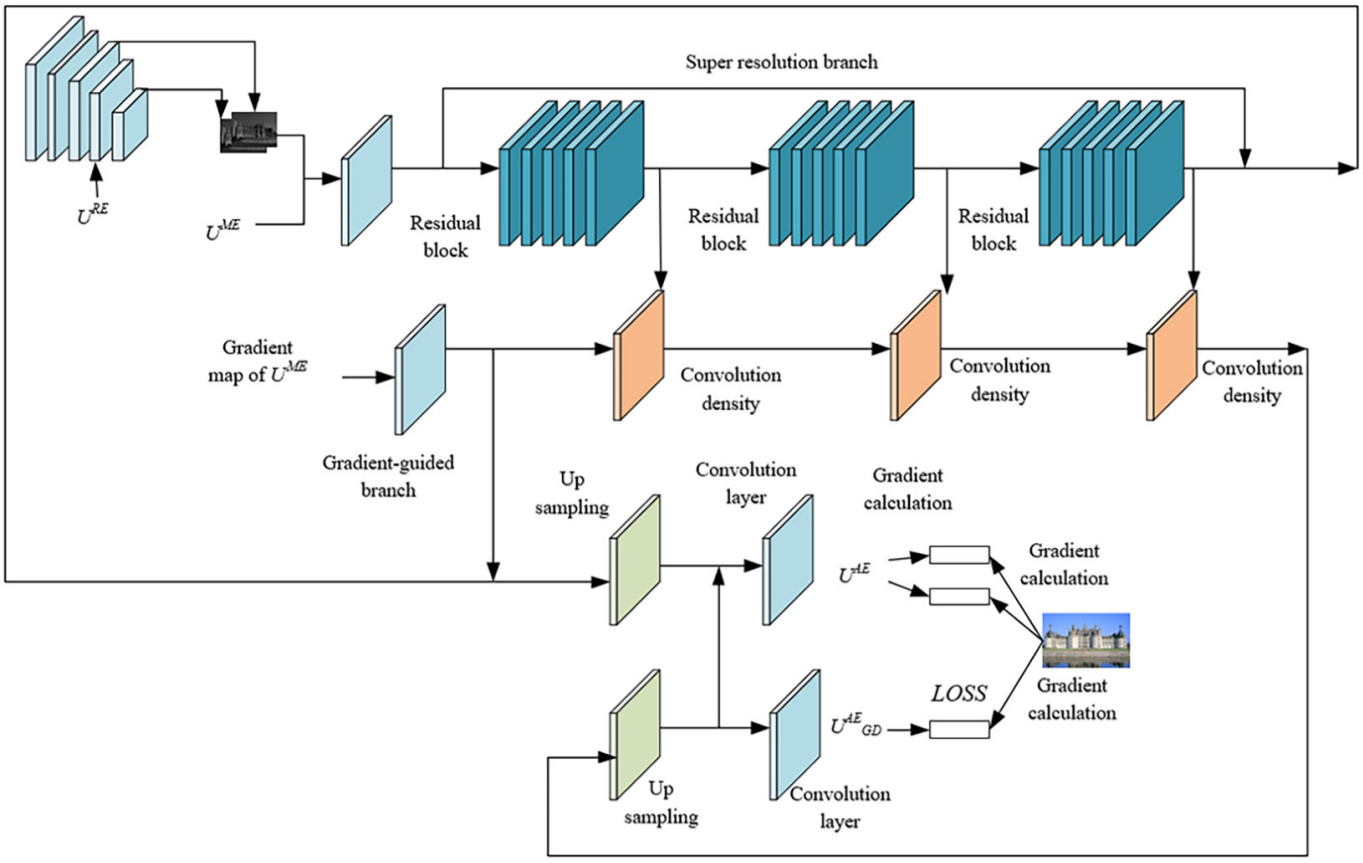

Fig. 4. Overall framework of the super-resolution network

When the reconstructed gradient map is attained, the network will adopt a two-way constraint strategy. On the one hand, the strategy uses the gradient of the original image to constrain and ensure consistency between the reconstructed image and the original image in the gradient direction; on the other hand, the strategy fuses with the intermediate features corresponding to the super-resolution branch to further improve the quality of the reconstructed image.

The specific calculation process is given below:
First, a gradient map H was attained based on following formulas:

$$U_z^{ME}(u,k) = U^{ME}(u+1,k) - U^{ME}(u,k) \tag{11}$$

$$U_t^{ME}(u,k) = U^{ME}(u,k+1) - U^{ME}(u,k) \tag{12}$$

$$H(u,k) = \sqrt{U_z^{ME}(z)^2 + U_t^{ME}(z)^2} \tag{13}$$

The constructed gradient branch network contains a convolution layer and nine residuals in the residual dense block (*RRDB*). Compared with the common residual block (*RB*), the structure of *RRDB* is deeper and denser, and this structure design can alleviate the common problem of gradient vanishing in deep networks. This is because in the process of back propagation, the gradient vanishing problem of deep networks can lead to training difficulties, and the design of dense connections can alleviate this problem to a certain extent.

To improve the overall accuracy of reconstructed image, $LOSS_{RE}$ was adopted to optimize the super-resolution branch, but since $LOSS_{RE}$ can produce blur details, the gradient loss $LOSS_{GR}$ was introduced together with $LOSS_{RE}$.

Assuming U_{GD} represents the reconstructed gradient of the gradient-guided branch, U_{GD}^{AE} represents the gradient of the reconstructed image of the super-resolution branch, and U_{GD}^{GE} represents the gradient of the original image, then the $LOSS_{GR}$ used to supervise the generation result of the gradient branch was calculated based on U_{GD} and U_{GD}^{GE}, the $LOSS_{SR}$ used to supervise the gradient of the reconstructed image of the super resolution branch was calculated based on U_{GD}^{AE} and U_{GD}^{GE}, and the final gradient loss function of the loss image was composed of $LOSS_{RE}$, $LOSS_{SR}$ and $LOSS_{GR}$; assuming β, α and ε are weighting coefficients, then there are:

$$LOSS_{RE} = \left\| U^{GE} - U^{AE} \right\|_1 \tag{14}$$

$$LOSS_{GR} = \left\| U_{GD} - U_{GD}^{GE} \right\|_1 \tag{15}$$

$$LOSS_{SR} = \left\| U_{GD}^{AE} - U_{GD}^{GE} \right\|_1 \tag{16}$$

$$LOSS = \beta LOSS_{RE} + \alpha LOSS_{GR} + \varepsilon LOSS_{SR} \tag{17}$$

4 EXPERIMENTAL RESULTS AND ANALYSIS

Table 1. PSS effect of different methods

Algorithm	Training Set	Test Set
	PSNR/SSIM/LPIPS	PSNR/SSIM/LPIPS
CNN-SR	24.926/0.725/0.473	31.957/0.851/0.298
AE-SR	26.347/0.731/0.147	32.956/0.851/0.1544
GAN-SR	23.786/0.778/0.159	30.856/0.861/0.084
SC-SR	27.269/0.854/0.272	33.836/0.825/0.184
The proposed algorithm	25.631/0.895/0.243	34.282/0.846/0.125

Table 1 lists the peak signal-to-noise ratio (*PSNR*), structural similarity index measure (*SSIM*), and learned perceptual image patch similarity (*LPIPS*) scores of some algorithms on the training set and test set. A higher *PSNR* score indicates a better effect of the algorithm; a higher *SSIM* score indicates a higher visual similarity between the reconstructed image and the original image; and a higher *LPIPS* score indicates better image quality. Comparative analysis shows that, on the training set, the *SC-SR* method performed the best in terms of *PSNR* and *SSIM*, but its performance on *LPIPS* was not as good, indicating that this method has some problems with detail restoration and image quality. On the test set, the proposed method outperformed other methods in terms of all three indicators, suggesting that the proposed method has excellent generalization ability on unseen data, and this also indicates that in an ILE, the proposed method could achieve a good effect with its advantages. For one thing, the proposed method plays a key role in enhancing the resolution of some specific regions around the high-resolution viewport; another is that the introduced gradient-guided branch can effectively reduce the false matching of high-resolution information through the guidance and adjustment of gradient prior information; and the image quality and visual effect could be further enhanced by indirectly constraining the high-frequency information of the reconstructed image.

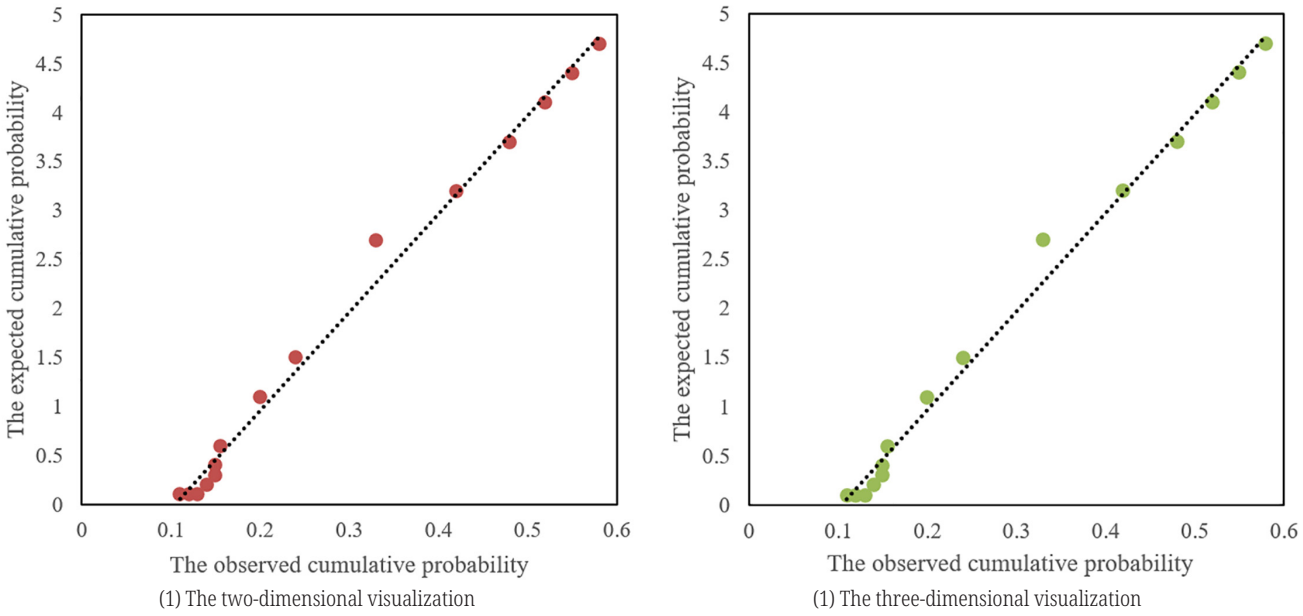

Fig. 5. *P-P* plots of normal distribution of students' immersive learning input

P-P plots can be used to verify whether a data set conforms to a certain theoretical distribution (such as a normal distribution) or not. In a *P-P* plot, if data points mostly fall near a line y = x, then it can be considered that the sample data conform to the theoretical distribution being examined. According to the data given in Figure 5, there is an overall convergence relation between the observed cumulative probability and the expected cumulative probability, and the data conform to the normal distribution to some extent. In most intervals, such as at positions of 0.14, 0.15–0.155, and 0.24–0.58, the observed values were closer to the expected values. Similarly, in the 3D visual layout, the students' immersive learning input approximately conforms to normal distribution. For students' immersive learning input of 3D visual layout, there are multiple influencing factors, so it's not just one simple normal distribution.

Table 2. Data of the first-round participation behavior analysis of immersive learning

Analysis Dimension		Proportion of Participation Behavior
Cognitive behavior	Problem-solving strategy	12.87%
	Information organization ability	6.52%
Emotional behavior	Learning motivation	0.22%
	Feeling of self-efficacy	22.89%
	Feeling of confusion	4.21%
	Feeling of satisfaction	12.7%
Social interaction behavior	Teamwork ability	24.65%
	Communication skill	11.6%
Skill behavior	Operation skill	0.48%
	Hand-eye coordination	3.86%

In this paper, students' learning behavior in an ILE was divided into four types, and a comparative experiment was carried out on students' participation in immersive learning within the designed framework of the learning environment. As can be known from Table 2, under the item of social interaction behavior, the score of teamwork ability was the highest, accounting for 24.65%, indicating that in the ILE, students' sense of cooperation was higher, they were good at completing tasks through collective collaboration, and this has also demonstrated our study, namely that the ILE can effectively enhance students' teamwork ability. Under the item of emotional behavior, the score of the sense of self-efficacy was higher, accounting for 22.89%, and this indicates that students' evaluation and trust of their own abilities were relatively high, which had a positive effect on encouraging students to actively participate in learning and challenge difficulties in the ILE. Under the item of cognitive behavior, the score of problem-solving strategy was relatively high as well, accounting for 12.87%, indicating that students can effectively use the said strategy to solve problems in the ILE. Overall speaking, the data show that in an ILE, students performed well in aspects of social interaction behavior, sense of self-efficacy, and problem-solving strategy. However, some aspects, such as learning motivation and operation skills need more of our attention so as to encourage students to develop in an all-round way in an immersive learning environment.

Table 3. Analysis results of students' participation level in immersive learning

Results of Paired t-Test						
Name	Analysis Dimension	Pair (Mean ± Standard Deviation)		Difference (Pair 1–Pair 2)	*t*	*P*
		Pair 1	Pair 2			
Pre-test versus post-test	Cognition dimension	41.28 ± 3.48	43.12 ± 4.35	–3.12	–4.128	0.000**
	Emotion dimension	37.18 ± 3.68	41.28 ± 3.65	–3.54	–4.875	0.000**
	Social interaction dimension	26.87 ± 2.47	26.48 ± 2.58	–1.89	–4.359	0.000**
	Skill dimension	21.05 ± 2.01	12.47 ± 21.62	–1.02	–4.211	0.000**
	Total score	97.26 ± 8.64	111.29 ± 8.68	–8.45	–8.642	0.000**

Notes: *$p < 0.05$; **$p < 0.01$.

According to the results of the paired t-test shown in Table 3, it's known that after the test, regardless of which dimension (cognition, emotion, social interaction, or skill), the scores of students had increased significantly, and all p-values were less than 0.01, which means that the changes were statistically significant; that is, the test had a significant influence on students' participation level in immersive learning. In terms of the cognition dimension, the post-test mean value of 43.12 was significantly higher than the pre-test mean value of 41.28; the difference was –3.12 and the t-value was –4.128. These results indicate that after the test, the students' cognition ability had been significantly enhanced. In terms of the emotion dimension, the post-test mean value of 41.28 was also significantly higher than the pre-test mean value of 37.18, which means that the test had a significant effect on increasing students' emotional input. In terms of the social interaction dimension, the post-test mean value showed a slight decrease from 26.87 to 26.48; the difference was –1.89, the t-value was –4.359, and the p-value was still less than 0.01, indicating that although the post-test scores were lower, overall speaking, the test still had a positive effect on enhancing students' social interaction ability. In terms of the skill dimension, after the test, the mean value increased from 21.05 to 21.62, the difference was –1.02, and the t-value was –4.211. These results could also prove the effect of the test on enhancing students' skill level. In terms of the total score, the post-test mean value of 111.29 was significantly higher than the pre-test mean value of 97.26; the difference was –8.45, and the t-test value was –8.642, which further confirms that the test had a positive effect on increasing students' participation in immersive learning. Overall speaking, the test could significantly improve the level of student participation in immersive learning in the four dimensions of cognition, emotion, social interaction, and skill, which means that the ILE can effectively contribute to the overall development of students.

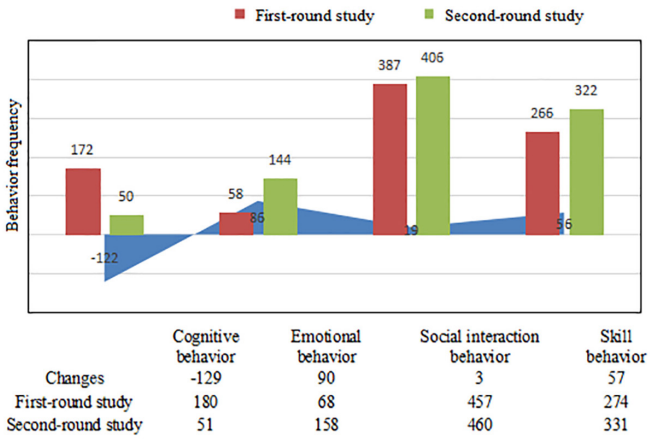

Fig. 6. Statistics of participation behavior frequency of immersive learning in each dimension

As can be seen from Figure 6, in the first-round and second-round studies, the participation behavior frequencies of the four dimensions (cognitive behavior, emotional behavior, social interaction behavior, and skill behavior) showed some changes. In the case of cognitive behavior, the behavior frequency decreased from 172 in the first round to 50 in the second round; the change was –122, indicating that the students' cognitive behavior was reduced in the second round of study, and this is because the students had gained some understanding of the ILE in this round, so the frequency of cognitive behavior decreased. The frequency of emotional behavior increased from 58 in the first round to 144 in the second round; the increment was 86, indicating that students' emotional input in the second round of study had obviously

increased. This is because students' experience of the ILE became deeper, so their positive emotions towards learning had enhanced. The frequency of social interaction behavior was 387 in the first round and 406 in the second round; the increment was 19, indicating that the students' social interaction ability had enhanced to some extent in the second round of study, this is because the students already got used to the ILE, and they began to conduct more social interactions. The frequency of skill behavior increased from 266 in the first round to 322 in the second round; the increment was 56, indicating that the frequency of students' skill behavior showed a significant increase in the second round of study. This is because they practiced constantly in the ILE and their operation skills had been improved. Overall speaking, with the launch of the ILE, students' emotional input, social interaction, and skill behavior increased, but their cognitive behavior decreased. This is because of their gradual familiarity with and adaptation to such an immersive learning environment.

5 CONCLUSION

The topic of this study is virtual reality and augmented reality for immersive learning: a framework of education environment design, and the content of the research includes the structural design of a super-resolution network and students' learning behavior in the ILE. In terms of super-resolution network structure, this paper proposes a super-resolution network comprising a gradient-guided branch and a super-resolution branch, which can adaptively fuse the content of a high-resolution viewport and improve the quality of edge details and the reconstructed image through the interactions between the gradient-guided branch and the super-resolution branch. Test results suggest that, compared with other methods, the proposed method has obvious advantages in terms of PSS effect.

In terms of students' learning behavior in the ILE, this paper gave a detailed analysis from four dimensions: cognitive behavior, emotional behavior, social interaction behavior, and skill behavior. Analysis results of students' participation behavior in the ILE show that the ILE can indeed significantly increase students' learning input and improve their learning effect. Research findings on the PSS effect and students' learning behavior in the ILE have both verified the effectiveness of the proposed method and provided new research perspectives and theoretical evidence for the design of the immersive learning environment.

In summary, this research explored the application of VR and AR technologies in the field of education, giving important insights into the design and research of immersive learning environments.

6 REFERENCES

[1] A. D. Samala, T. Usmeldi, Y. Daineko, Y. Indarta, Y. A. Nando, M. Anwar, P. Jaya, and Almasri, "Global publication trends in augmented reality and virtual reality for learning: The last twenty-one years," *International Journal of Engineering Pedagogy*, vol. 13, no. 2, pp. 109–128, 2023. https://doi.org/10.3991/ijep.v13i2.35965

[2] I. Phelan, P. J. Furness, M. Matsangidou, N. T. Babiker, O. Fehily, A. Thompson, A. Carrion-Plaza, and S. A. Lindley, "Designing effective virtual reality environments for pain management in burn-injured patients," *Virtual Reality*, vol. 27, no. 1, pp. 201–215, 2023. https://doi.org/10.1007/s10055-021-00552-z

[3] G. Al Farsi, A. M. Yusof, A. Romli, R. M. Tawafak, S. I. Malik, J. Jabbar, and M. E. B. Rsuli, "A review of virtual reality applications in an educational domain," *International Journal of Interactive Mobile Technologies*, vol. 15, no. 22, pp. 99–110, 2021. https://doi.org/10.3991/ijim.v15i22.25003

[4] M. Bhatia, P. Manani, A. Garg, S. Bhatia, and R. Adlakha, "Mapping mindset about gamification: Teaching learning perspective in UAE education system and Indian education system," *Revue d'Intelligence Artificielle*, vol. 37, no. 1, pp. 47–52, 2023. https://doi.org/10.18280/ria.370107

[5] M. Sabree and M. M. Mustafa, "Importance and role of live projects in architectural education using a descriptive and analytical approach," *Education Science and Management*, vol. 1, no. 1, pp. 7–18, 2023. https://doi.org/10.56578/esm010102

[6] A. Reyad, L. Almazaydeh, A. Bilal and K. Elleithy, "Information technology students' perceptions toward using virtual reality technology for educational purposes," *International Journal of Interactive Mobile Technologies*, vol. 17, no. 7, pp. 148–166, 2023. https://doi.org/10.3991/ijim.v17i07.37211

[7] Y. V. Tsekhmister, T. Konovalova, B. Y. Tsekhmister, A. Agrawal, and D. Ghosh, "Evaluation of virtual reality technology and online teaching system for medical students in Ukraine during COVID-19 pandemic," *International Journal of Emerging Technologies in Learning*, vol. 16, no. 23, pp. 127–139, 2021. https://doi.org/10.3991/ijet.v16i23.26099

[8] P. Yang and Z. Liu, "The Influence of Immersive Virtual Reality (IVR) on skill transfer of learners: The moderating effects of learning engagement," *International Journal of Emerging Technologies in Learning*, vol. 17, no. 10, pp. 62–73, 2022. https://doi.org/10.3991/ijet.v17i10.30923

[9] A. Kleftodimos, A. Evagelou, A. Triantafyllidou, M. Grigoriou, and G. Lappas, "Location-based augmented reality for cultural heritage communication and education: The Doltso district application," *Sensors*, vol. 23, no. 10, p. 4963, 2023. https://doi.org/10.3390/s23104963

[10] Septinaningrum, K. A. Hakam, W. Setiawan, and M. Agustin, "Developing of augmented reality media containing Grebeg Pancasila for character learning in elementary school," *Ingénierie des Systèmes d'Information*, vol. 27, no. 2, pp. 243–253, 2022. https://doi.org/10.18280/isi.270208

[11] C. Papakostas, C. Troussas, A. Krouska, and C. Sgouropoulou, "Exploring users' behavioral intention to adopt mobile augmented reality in education through an extended technology acceptance model," *International Journal of Human–Computer Interaction*, vol. 39, no. 6, pp. 1294–1302, 2023. https://doi.org/10.1080/10447318.2022.2062551

[12] F. Sukmawati, E. B. Santosa, and T. Rejekiningsih, "Design of virtual reality zoos through Internet of Things (IoT) for student learning about wild animals," *Revue d'Intelligence Artificielle*, vol. 37, no. 2, pp. 483–492, 2023. https://doi.org/10.18280/ria.370225

[13] T. Seyman Guray and B. Kismet, "Applicability of a digitalization model based on augmented reality for building construction education in architecture," *Construction Innovation*, vol. 23, no. 1, pp. 193–212, 2023. https://doi.org/10.1108/CI-07-2021-0136

[14] M. Leißau, S. Hellbach, and C. Laroque, "Self-paced learning in virtual worlds: Opportunities of an immersive learning environment," In *20th European Conference on e-Learning (ECEL)*, pp. 257–265, 2021. https://doi.org/10.34190/EEL.21.053

[15] H. Lin and M. Pryor, "Student intrinsic-motivational perceptions on a 3D immersive learning environment," in *IEEE International Conference on Educational Technology (ICET)*, Beijing, China, pp. 167–171, 2021. https://doi.org/10.1109/ICET52293.2021.9563100

[16] T. Onorati, P. Diaz, T. Zarraonandia, and I. Aedo, "Exploring a multi-device immersive learning environment," in *Proceedings of the 2022 International Conference on Advanced Visual Interfaces*, Rome Italy, pp. 1–3, 2022. https://doi.org/10.1145/3531073.3534485

[17] Y. Jia and R. Qi, "Influence of an immersive virtual environment on learning effect and learning experience," *International Journal of Emerging Technologies in Learning*, vol. 18, no. 6, pp. 83–95, 2023. https://doi.org/10.3991/ijet.v18i06.37815

[18] Y. D. Barve, P. Patil, A. Bhattacharjee, and A. Gokhale, "Pads: Design and implementation of a cloud-based, immersive learning environment for distributed systems algorithms," *IEEE Transactions on Emerging Topics in Computing*, vol. 6, no. 1, pp. 20–31, 2017. https://doi.org/10.1109/TETC.2017.2731984

[19] D. Abbott, S. Jeffrey, A. Gouseti, K. Burden, and M. Maxwell, "Development of cross-curricular key skills using a 3D immersive learning environment in schools," in *Proceedings 3, Immersive Learning Research Network: Third International Conference, iLRN 2017*, Coimbra, Portugal, pp. 60–74, 2017. https://doi.org/10.1007/978-3-319-60633-0_6

[20] Y. D. Barve, P. Patil, and A. Gokhale, "A cloud-based immersive learning environment for distributed systems algorithms," in *IEEE 40th Annual Computer Software and Applications Conference (COMPSAC)*, Atlanta, GA, USA, vol. 1, pp. 754–763, 2016. https://doi.org/10.1109/COMPSAC.2016.26

[21] Z. Chen, "Computer graphics image and visual communication design model in computer VR environment," in *IEEE Conference on Telecommunications, Optics and Computer Science (TOCS)*, Dalian, China, pp. 1356–1360, 2022. https://doi.org/10.1109/TOCS56154.2022.10016091

[22] Z. Bing and Z. Qian, "Visual imaging method of 3D virtual scene based on VR technology," in *Proceedings, Part II 3 Multimedia Technology and Enhanced Learning: Third EAI International Conference, ICMTEL 2021, Virtual Event*, pp. 373–384, 2021. https://doi.org/10.1007/978-3-030-82565-2_31

[23] T. Tsunajima and N. Nishiuchi, "Visual environment design of VR space for sequential reading in web browsing," in *Proceedings, Part II 22 HCI International 2020-Posters: 22nd International Conference, HCII 2020*, Copenhagen, Denmark, pp. 131–136, 2020. https://doi.org/10.1007/978-3-030-50729-9_18

[24] Y. Tongpaeng and P. Kewirat, "Design educational VR application through TPACK Model: A case study of basic scientific experiment for secondary school students in Thailand," in *6th International Conference on Information Technology (InCIT)*, pp. 270–274, 2022. https://doi.org/10.1109/InCIT56086.2022.10067609

[25] R. Frieß, T. Voigt, F. Gnadlinger, C. Holtmann, and M. Steinicke, "Design-based research on a cooperative educational VR game about OHM's law," in *ECGBL 2021 15th European Conference on Game-Based Learning*, p. 233, 2021. https://doi.org/10.34190/GBL21.134

7 AUTHOR

Biqin Yang has completed Ph.D in international economics, and has graduated from Southwestern University of Finance and Economics in China. She is currently is an educator and serving as Vice Professor at Minnan Normal University in China. She has published 30 papers and 4 books so far (E-mail: yangbiqin1987@163.com; ORCID: https://orcid.org/0009-0009-0242-1419).